[2] Wheeler, P. C., "Spinning Spacecraft Attitude Control via the Environmental Magnetic Field," *Journal of Spacecraft and Rockets*, Vol. 4, No. 12, Dec. 1967, pp. 1631–1637.

[3] Vrablik, E. A., Black, W. L., and Travis, L. J., "LES-4 Spin Axis Orientation System," TN 1965-48, 1965, Lincoln Lab., Massachusetts Institute of Technology, Cambridge, Mass.

[4] Fischell, R. E., "Spin Control for Earth Satellites," *Peaceful Uses of Automation in Outer Space*, edited by J. A. Aseltine, Plenum Press, New York, 1966, pp. 211–218.

[5] Sonnabend, D., "A Magnetic Control System for an Earth Pointing Satellite," *Proceedings of the Symposium on Attitude Stabilization and Control of Dual-Spin Spacecraft*, Rept. TR-0158(3307-01)-16, Nov. 1967, Aerospace Corp., El Segundo, Calif., pp. 121–144.

[6] Hecht, E., and Manger, W. P., "Magnetic Attitude Control of the TIROS Satellites," *Torques and Attitude Sensing in Earth Satellites*, edited by S. Fred Singer, Academic Press, New York, 1964, pp. 127–135.

[7] Yu, E. Y., "Spin Decay, Spin-Precession Damping, and Spin-Axis Drift of the Telstar Satellite," *Bell System Technical Journal*, Vol. 42, No. 5, Sept. 1963, pp. 2169–2193.

[8] Sorensen, J. A., "Precision Magnetic Attitude Control of Spinning Spacecraft," SUDAAR 380, Aug. 1969, Dept. of Aeronautics and Astronautics, Stanford Univ., Stanford, Calif.

[9] Lange, B. O., Fleming, A. W., and Parkinson, B. W., "Control Synthesis for Spinning Aerospace Vehicles," *Journal of Spacecraft and Rockets*, Vol. 4, No. 2, Feb. 1967, pp. 142–150.

[10] Bryson, A. E. and Ho, Y. C., *Applied Optimal Control*, Blaisdell Publishing Co., Waltham, Mass., 1969, pp. 148–176.

[11] Moore, J. B. and Anderson, B. D. O., "Generalizations of the Circle Criterion," TR EE-6708, Oct. 1967, Dept. of Electrical Engineering, Univ. of Newcastle, New South Wales, Australia.

MAY 1971 J. SPACECRAFT VOL. 8, NO. 5

Semipassive and Active Nutation Dampers for Dual-Spin Spacecraft

D. L. MINGORI,* J. A. HARRISON,† AND G. T. TSENG†
University of California, Los Angeles, Calif.

The acquisition of flight data from orbiting dual-spin spacecraft has emphasized the difficulty of providing assurance that dissipative effects tending to reduce nutation outweigh those tending to increase it. Although passive platform-mounted devices for attenuating nutation are generally reliable and conceptually simple, their effectiveness may be limited. This paper is concerned with alternative devices, namely, single-axis control moment gyros (CMG's) whose rotational motion relative to the spacecraft is either a) restrained passively by a spring and dashpot, or b) controlled actively by a torque motor driven with sensed information from a rectilinear accelerometer. Although the passively controlled device can operate effectively only when placed on the platform, the active device can be effective when placed on the rotor as well. Both devices are capable of reducing nutation several times faster than passive dampers of equal mass.

Nomenclature

$\mathbf{a}^P$ = acceleration of P, Eq. (32)
a_m = measured component of $\mathbf{a}^P$, Eq. (33)
B,B' = two primary bodies of spacecraft
c = CMG gimbal damping constant
$\mathbf{d}$ = $\sum_{i=1}^{3} d_i\mathbf{x}_i$, position vector from system cm to CMG cm
e_a = armature voltage
f = tuning factor, Eq. (31)
$\mathbf{h}_g$ = CMG angular momentum
h = magnitude of $\mathbf{h}_g$, Eq. (29)
i_a = armature current
I_i = moment of inertia of B plus B' for X_i
I_3' = moment of inertia of B' for X'_3
$[\bar{I}_1,\bar{I}_2,\bar{I}_3]$ = $[I_1 + m(d_2^2 + d_3^2), I_2 + m(d_1^2 + d_3^2), I_3 + m(d_1^2 + d_2^2)]$
J_1,J_3 = centroidal principal moments of inertia of CMG wheel for transverse and symmetry axes, respectively
J_m = motor rotor moment of inertia
K = combined gain of accelerometer and amplifier
K_e = back emf of motor
K_T = torque constant of motor
k = semipassive CMG spring constant
m = mass of CMG
$\mathbf{M}_t$ = $\sum_{i=1}^{2} M_i\mathbf{x}_i$, transverse reaction torque applied to B by CMG
p = passive CMG natural frequency, Eq. (9b)
$\mathbf{p}$ = $\sum_{i=1}^{3} p_i\mathbf{x}_i$, position vector from system cm to accelerometer
P = power consumed by CMG torque motor
P_{ave} = average value of P
R_a = armature resistance
r = ratio of transverse inertias, Eq. (3c)
$\mathbf{T}$ = $\sum_{i=1}^{3} T_i\mathbf{x}_i$, torque applied to CMG
$\mathbf{x}_i$ = unit vector parallel to X_i
X_1,X_2,X_3 = reference axes fixed in B and passing through system cm
X_3' = symmetry axis of B'
β = motor friction constant combining effects of viscous friction and back emf
γ = gimbal angle, Fig. 1
γ_0 = steady-state amplitude of γ, Eqs. (15) and (42)
Δ = measure of gyro size, Eq. (3c)
ζ = passive CMG damping ratio, Eq. (9b)
η,ν = Eq. (3d) and (9a), respectively
λ_1,λ_2 = Eqs. (3a,b)

Received August 7, 1970; revision received November 20 1970.

* Assistant Professor, School of Engineering and Applied Science. Member AIAA.

† Graduate Student, School of Engineering and Applied Science.

λ = nutation frequency as seen on B for symmetric spacecraft, Eq. (10)
Λ = $I_3'\sigma/\bar{I}_1'$
ρ = ratio of motor speed to $\dot{\gamma}$ (values of ρ different from one reflect the presence of a gear train.)
σ = constant angular speed of B' relative to B
Σ = constant angular speed of CMG wheel relative to gimbal
τ_0 = time constant of lag compensation
ϕ = steady-state phase angle, Eqs. (16) and (43)
ω_i = measure number of inertial angular velocity of B for X_i
ω_N = $(\lambda_1\lambda_2)^{1/2}$, nutation frequency as seen on B
ω_t,ω_l = transverse component of inertial angular velocity of B
Ω = nominal inertial angular speed of B for X_3

Introduction

PREVIOUS investigations of the dynamics of dual-spin spacecraft[1-4] have indicated that if the moment of inertia of the rotor for its symmetry axis is less than the moment of inertia of the entire spacecraft for a centroidal transverse axis, then energy dissipation on the rotor has a destabilizing effect, whereas energy dissipation on the platform has a stabilizing effect. In theory, the simplest way to assure spacecraft stability is to mount on the platform a passive damping mechanism[5,6] that will respond to coning of the rotor spin axis, i.e., nutation, by dissipating energy in much greater quantities than all of the sources of rotor dissipation combined. A specific mechanization consisting of a proof mass oscillating on the end of an elastic wire and encased in a container of viscous fluid has been employed in space. Such devices have almost unlimited lifetimes, require no power, and are conceptually simple. However, they have some shortcomings in that a) present analytical and experimental capabilities are not sufficiently refined to make possible the accurate prediction or measurement of energy dissipation on the rotor as a function of nutation angle (this information is required in order to design a sufficiently effective platform damper); and b) increased effectiveness of a passive platform damper must normally be achieved at the cost of increased mass or increased distance from the mass center. These propositions may be unacceptable when a substantial factor of safety is required in the damper design because of uncertainties associated with rotor dissipation.

This paper is concerned with alternative approaches. A device employing an actively controlled mass particle has been studied by Kane and Scher.[7] The specific alternatives considered here include a semipassive device consisting of a single-axis control moment gyro (CMG) whose rotational motion relative to the spacecraft is restrained by a spring and dashpot, and an active device consisting of a single-axis CMG whose rotational motion is controlled by a torque motor driven with sensed information from a single-axis translational accelerometer.

Description of the System

The idealized system to be examined consists of two rigid bodies B and B' whose relative motion is restricted to rotation about an axis X_3' fixed in both bodies (see Fig. 1). It is assumed that X_3' is an axis of inertial symmetry for B', and that a despin motor maintains a constant relative speed σ between the two bodies.

A single-degree-of-freedom CMG whose mass center lies on its gimbal axis is mounted on B in such a way that gimbal rotation can take place only about an axis perpendicular to X_3'. The introduction of three additional axes X_1, X_2, and X_3 facilitates the writing of differential equations of motion for this system. These axes, mutually perpendicular and right-handed, are fixed in B and pass through the mass center of the entire system (also fixed in B); X_1 is parallel to the gimbal axis of the gyro, and X_3 is parallel to X_3'. To simplify the analysis, it will be assumed that when the gyro spin axis is parallel to X_3, then X_1, X_2, and X_3 become centroidal principal axes of the entire spacecraft.

Two modes of operation will be considered. In one, rotation of the CMG gimbal relative to B is resisted by a linear spring and dashpot, whereas in the other such motion is controlled by a torque motor. In both cases, the nominal orientation of the CMG spin axis is parallel to X_3. Three system equations which govern the motion in both modes can be obtained by applying the angular momentum principle to the entire spacecraft. For semipassive operation (using a spring and dashpot), an additional gyro equation can be obtained by applying the angular momentum principle to the CMG alone and using the X_1 component of the resulting vector equation. For active operation, a control law using sensed information (in this case from a translational accelerometer) must be specified.

Nonlinear versions of the system equations are given in the Appendix. Effects of external torques have been neglected. The nonlinear system equations together with appropriate gyro equations may be integrated on a computer to check the predictions of simplified analyses. They are too complicated, however, to analyze directly. Linearized equations will be used for this purpose. It may be verified by substitution that the system equations are satisfied by setting

$$\omega_1 = \omega_2 \equiv 0; \qquad \gamma \equiv 0,\ \omega_3 \equiv \Omega, \text{ a constant} \tag{1}$$

[We shall later see that the gyro equations also are satisfied by Eq. (1).] Dropping nonlinear terms in the small quantities ω_1, ω_2, γ and their derivatives, we obtain

$$(\bar{I}_1 + J_1)\dot{\omega}_1 + [(\bar{I}_3 + J_3 - \bar{I}_2 - J_1)\omega_3 + I_3'\sigma + J_3\Sigma]\omega_2 = -J_1\ddot{\gamma} - [(J_3 - J_1)\omega_3 + J_3\Sigma]\omega_3\gamma \tag{2a}$$

$$(\bar{I}_2 + J_1)\dot{\omega}_2 - [(\bar{I}_3 + J_3 - \bar{I}_1 - J_1)\omega_3 + I_3'\sigma + J_3\Sigma]\omega_1 = [(J_3 - 2J_1)\omega_3 + J_3\Sigma]\dot{\gamma} \tag{2b}$$

$$(\bar{I}_3 + J_3)\dot{\omega}_3 = 0 \tag{2c}$$

Solution of Eq. (2c) gives $\omega_3 = \Omega$. This solution can be substituted into Eqs. (2a) and (2b) to obtain linear equations with constant coefficients. Let

$$\lambda_1 \equiv [(\bar{I}_3 + J_3 - \bar{I}_2 - J_1)\Omega + I_3'\sigma + J_3\Sigma]/(\bar{I}_1 + J_1) \tag{3a}$$

$$\lambda_2 \equiv [(\bar{I}_3 + J_3 - \bar{I}_1 - J_1)\Omega + I_3'\sigma + J_3\Sigma]/(\bar{I}_2 + J_1) \tag{3b}$$

$$\Delta \equiv J_1/(\bar{I}_1 + J_1); \quad r \equiv (\bar{I}_1 + J_1)/(\bar{I}_2 + J_1) \tag{3c}$$

$$\eta \equiv J_3(\Omega + \Sigma)/(\bar{I}_1 + J_1) \tag{3d}$$

λ_1 and λ_2 are frequency-like quantities related to the nutation frequency ω_N as seen on B according to the equation $\omega_N = (\lambda_1\lambda_2)^{1/2}$. Δ reflects the size of the gyro as compared to that of the entire spacecraft; r is a measure of the inertial symmetry of B; and η represents the gyro angular momentum divided by the transverse moment of inertia of the entire spacecraft. In terms of these parameters, the two system equations governing the coning motion of X_3, Eqs. (2a) and (2b) can be written as

$$\dot{\omega}_1 + \lambda_1\omega_2 = -\Delta\ddot{\gamma} - (\eta - \Delta\Omega)\Omega\gamma \tag{4a}$$

$$\dot{\omega}_2 - \lambda_2\omega_1 = r(\eta - 2\Delta\Omega)\dot{\gamma} \tag{4b}$$

Before proceeding further, the preceding equations must be augmented with the appropriate gyro equation.

Semipassive CMG Damper

Suppose a linear torsional spring with spring constant k and a linear torsional dashpot with damping constant c are installed between the CMG gimbal and body B in such a way that the inter-body torque $\mathbf{T}$ applied to the CMG about its

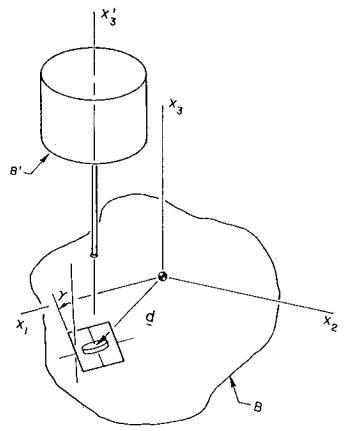

Fig. 1 Dual-spin system with CMG.

mass center satisfies

$$T_1 = \mathbf{T}\cdot\mathbf{x}_1 = -k\gamma - c\dot{\gamma} \tag{5}$$

where $\mathbf{x}_1$ is a unit vector directed along X_1. Using $\mathbf{h}_g$ to denote the angular momentum of the gyro for its mass center one can write

$$d\mathbf{h}_g/dt = \mathbf{T} \tag{6}$$

After introducing the appropriate expression for $\mathbf{h}_g$, dot multiplying both sides of Eq. (6) with $\mathbf{x}_1$, and substituting from Eq. (5), one obtains

$$J_1(\dot{\omega}_1 + \ddot{\gamma}) + (\omega_2\cos\gamma + \omega_3\sin\gamma)(-\omega_2\sin\gamma + \omega_3\cos\gamma)(J_3 - J_1) + (\omega_2\cos\gamma + \omega_3\sin\gamma)\Sigma J_3 = -k\gamma - c\dot{\gamma} \tag{7}$$

This equation completes the set required to describe the behavior of the semipassively damped system. Noting that the solution given in Eq. (1) also satisfies Eq. (7), we linearize the latter equation as before:

$$\ddot{\gamma} + 2\zeta p\dot{\gamma} + p^2\gamma = -\dot{\omega}_1 - \nu\omega_2 \tag{8}$$

where

$$\nu \equiv [\Omega(J_3 - J_1) + \Sigma J_3]/J_1 \tag{9a}$$

$$p^2 \equiv (k/J_1) + \Omega\nu; \quad 2\zeta p \equiv c/J_1 \tag{9b}$$

Equations (4a, 4b, and 8) describe the motion of the spacecraft in the neighborhood of the nominal motion; they are linear and have constant coefficients, so that well-known methods can be used to study their solutions. However, we will present an approximate reaction torque analysis first, to provide a) insight into the behavior of the system, and b) a convenient starting point for the discussion of actively controlled CMG's.

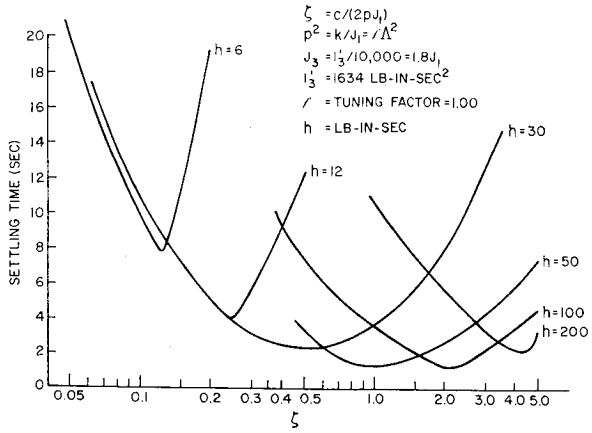

Fig. 2 Minimum settling times.

Reaction Torque Analysis

The right-hand sides of Eqs. (4a-b) may be thought of as torques applied to the spacecraft by the CMG for the axes X_1 and X_2. As a first step in the reaction torque argument, one assumes that these torques are small and solves Eqs. (4a-b), considering the right-hand sides to be zero. Since these arguments are approximate already, little is lost by making the further simplifying assumption that X_3 is an axis of inertial symmetry for the spacecraft so that

$$\lambda_1 = \lambda_2 = \lambda, \quad r = 1 \tag{10}$$

The solutions of the truncated versions of Eqs. (4a-b) can then be written as

$$\omega_1 = \omega_t\sin\lambda t; \quad \omega_2 = -\omega_t\cos\lambda t \tag{11}$$

where ω_t is the magnitude of the transverse component of the angular velocity of B. Using Eq. (11) to express the driving terms on the right-hand side of Eq. (8) as explicit functions of time, one obtains

$$\ddot{\gamma} + 2\zeta p\dot{\gamma} + p^2\gamma = -\omega_t(\lambda - \nu)\cos\lambda t \tag{12}$$

which has the steady-state solution

$$\gamma = \gamma_0\cos(\lambda t - \phi) \tag{13}$$

where

$$\gamma_0 = \omega_t(\nu - \lambda)[(p^2 - \lambda^2)^2 + 4\zeta^2p^2\lambda^2]^{-1/2} \tag{14}$$

$$\phi = \tan^{-1}[2\zeta p\lambda/(p^2 - \lambda^2)] \tag{15}$$

The moments applied to the spacecraft by the gyro, neglected earlier to obtain approximate solutions for ω_1 and ω_2, can now be expressed as functions of time by substituting Eqs. (13–15) into the right-hand sides of Eqs. (4a-b):

$$M_1 = -\Delta\ddot{\gamma} - (\eta - \Delta\Omega)\Omega\gamma = [\Delta\lambda^2 - \Omega(\eta - \Delta\Omega)]\gamma_0\cos(\lambda t - \phi) \tag{16a}$$

$$M_2 = (\eta - 2\Delta\Omega)\dot{\gamma} = -(\eta - 2\Delta\Omega)\lambda\gamma_0\sin(\lambda t - \phi) \tag{16b}$$

where M_1 and M_2 are the applied torques for the axes X_1 and X_2, respectively. The effect of these torques on $\boldsymbol{\omega}_t$ can be studied by considering the average value of $\mathbf{M}_t\cdot\boldsymbol{\omega}_t$. Using Eqs. (11), (16a–b), and a set of unit vectors $\mathbf{x}_1, \mathbf{x}_2, \mathbf{x}_3$ directed along X_1, X_2, and X_3, respectively, one obtains

$$\mathbf{M}_t\cdot\boldsymbol{\omega}_t = (M_1\mathbf{x}_1 + M_2\mathbf{x}_2)\cdot(\omega_1\mathbf{x}_1 + \omega_2\mathbf{x}_2) = M_1\omega_1 + M_2\omega_2 = [\Delta\lambda^2 - \Omega(\eta - \Delta\Omega)]\gamma_0 \times (\cos\lambda t\cos\phi + \sin\lambda t\sin\phi)\omega_t\sin\lambda t + (\eta - 2\Delta\Omega)\lambda\gamma_0(\sin\lambda t\cos\phi - \cos\lambda t\sin\phi)\omega_t\cos\lambda t \tag{17}$$

By expansion in a Fourier series it can be shown that the average value of the preceding periodic function is

$$(\mathbf{M}_t\cdot\boldsymbol{\omega}_t)_{\text{ave}} = \{\omega_t\gamma_0(\lambda + \Omega)[\Delta(\lambda + \Omega) - \eta]\sin\phi\}/2 \tag{18}$$

By substituting the definitions of γ_0, Δ, and η into this expression, one obtains (after some manipulation)

$$(\mathbf{M}_t\cdot\boldsymbol{\omega}_t)_{\text{ave}} = -\frac{\omega_t^2\Delta(\nu - \lambda)^2(\lambda + \Omega)}{2[(p^2 - \lambda^2)^2 + 4\zeta^2p^2\lambda^2]^{1/2}}\sin\phi \tag{19}$$

To reduce nutation, it is necessary that $(\mathbf{M}_t\cdot\boldsymbol{\omega}_t)_{\text{ave}}$ be negative, i.e., that $\mathbf{M}_t$ oppose $\boldsymbol{\omega}_t$ on the average. It is desirable that this product be large in magnitude as well. We shall now consider the extent to which this is possible when the CMG damper is placed on the platform and on the rotor.

Damper on the Platform

In studying the behavior of damping mechanisms on spinning and dual-spin satellites, it is important to determine the sign of λ, the nutation frequency as seen on the body con-

taining the damper. The designation of B as the platform means that for the nominal motion, $\Omega = 0$. With regard to σ, it is assumed without loss of generality that $\sigma > 0$. Furthermore, it is assumed that although the gyro spin rate is much greater than the rotor spin rate, the gyro angular momentum is much less than the rotor angular momentum because of the differences in spin axis inertias.

An attractive feature of the dual-spin concept is the possibility of designing a well-behaved system even when X_3 is not the axis of greatest inertia. Taking advantage of this feature and using the spin rate conditions just stated, one is led to the conclusion that $\lambda > 0$ when B is the platform [see Eqs. (3) and (10)].

A physical interpretation of Eq. (15) shows that when $\lambda > 0$, ϕ varies between 0° and 180°, and hence $\sin\phi > 0$. Using this relationship and the observations that $\Omega = 0$ and $\lambda > 0$, we conclude that

$$(\mathbf{M}_t \cdot \boldsymbol{\omega}_t)_{\text{ave}} < 0 \tag{20}$$

when the damper is on the platform. Interpreting this fact physically, we observe that the inter-body torque applied by the gyro to the platform opposes the transverse angular rate on the average and tends, therefore, to reduce nutation.

To maximize the effectiveness of the damper, we must select parameter values that make $(\mathbf{M}_t \cdot \boldsymbol{\omega}_t)_{\text{ave}}$ large in magnitude. This topic is discussed later; at this point one can only say that a CMG damper placed on the platform appears to be a promising candidate for a nutation damping device.

Damper on the Rotor

Here we consider B to be the rotor and B' to be the platform. In cases of practical interest, X_3' would normally coincide with X_3. In order that B' have zero inertial rate in the nominal motion, we require that $\sigma = -\Omega$. In addition, we assume as before that the spin rate of the rotor (in this case Ω) is positive, the gyro angular momentum is much smaller than the rotor angular momentum, and X_3 is a centroidal principal axis of minimum moment of inertia for the spacecraft. Then, when B is considered as the rotor, λ as seen on B satisfies

$$-\Omega < \lambda < 0 \tag{21}$$

[See Eqs. (3) and (10).] For negative λ, the phase angle ϕ varies between 180° and 360°, so that $\sin\phi < 0$. The use of this condition and Eqs. (19) and (21) yields the inequality

$$(\mathbf{M}_t \cdot \boldsymbol{\omega}_t)_{\text{ave}} > 0 \tag{22}$$

Hence, a CMG damper mounted on the rotor produces an inter-body torque that tends to increase nutation. This conclusion, and also the previous conclusion regarding the CMG damper on the platform, agrees with the accepted notion on the behavior of damping mechanisms that are not actively controlled. Namely, such mechanisms will tend to stabilize the spacecraft if placed on the platform and destabilize it if placed on the rotor.[1-4] In thinking ahead to a topic discussed in a later section, it may be mentioned that the ability to actively control the gimbal angle will make it possible to keep $(\mathbf{M}_t \cdot \boldsymbol{\omega}_t)_{\text{ave}}$ negative regardless of the location of the CMG.

Linearized Analysis and Nonlinear Verification

The linearized vehicle Eqs. (4a, 4b, and 8) will now be used to study the behavior of a specific system with a platform-mounted CMG damper. Employing the standard techniques for studying the solutions of constant coefficient linear equations, we first write the characteristic equation as

$$s^4 + a_3 s^3 + a_2 s^2 + a_1 s + a_0 = 0 \tag{23}$$

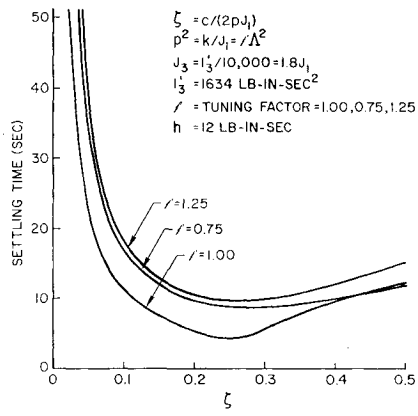

Fig. 3 Variations in tuning ratio.

where

$$a_3 = 2p\zeta/(1 - \Delta) \tag{24}$$

$$a_2 = [p^2 + \lambda_1\lambda_2 - \Delta\nu(\Omega + \lambda_2) + r\Delta(\nu - \Omega)(\nu - \lambda_1)]/(1 - \Delta) \tag{25}$$

$$a_1 = 2\zeta p\lambda_1\lambda_2/(1 - \Delta) \tag{26}$$

$$a_0 = [p^2\lambda_1\lambda_2 - \Delta\nu^2\Omega\lambda_2]/(1 - \Delta) \tag{27}$$

The roots of Eq. (23) will all lie in the left half of the complex plane if and only if the following inequalities are satisfied:

$$p^2 + \Delta[\lambda_1\lambda_2 - \nu(\Omega + \lambda_2) + r(\nu - \Omega)(\nu - \lambda_1)] > 0 \tag{28a}$$

$$(\nu - \lambda_1)\lambda_2[-\lambda_1\lambda_2 + \nu\Omega + r(\nu - \Omega)\lambda_1] > 0 \tag{28b}$$

$$p^2\lambda_1\lambda_2 - \Delta\nu^2\Omega\lambda_2 > 0 \tag{28c}$$

As discussed earlier, a nutation damper of the type under consideration only functions effectively when placed on the despun platform. These inequalities can be shown to verify this conclusion for realistic parameter values. For a platform-mounted damper, inequalities (28a-c) may be simplified somewhat by setting $\Omega = 0$. Still, these inequalities remain too complicated to yield much information directly. Furthermore, they can at best define conditions under which stability is assured, and do not help one to select the system that performs best from among all stable systems. For these reasons, a computer program that computes the eigenvalues of the characteristic equation [Eq. (23)] is employed to study system performance.

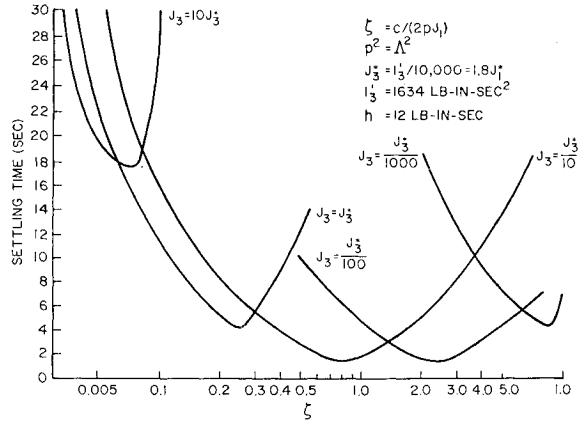

Fig. 4 Variations in gyro inertia with gyro momentum constant.

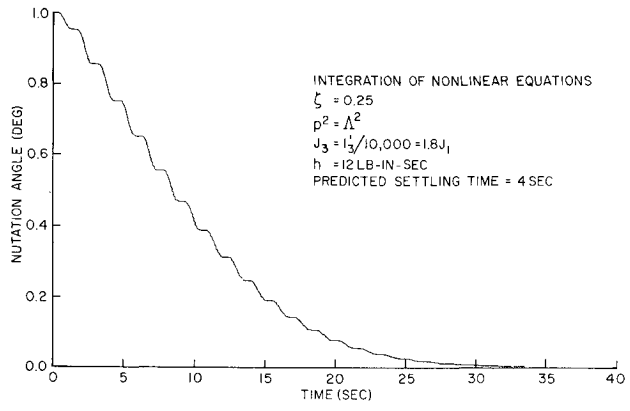

Fig. 5 Attenuation of nutation: semipassive system.

The index of performance used in the following discussion is the settling time, i.e., the time required for the response to a disturbance of the system to be reduced by a factor of $1/e$. For stable systems, this may be calculated as the negative of the reciprocal of the real part of the characteristic root nearest the imaginary axis.

Suppose the mass properties and spin rates of B and B' are given and cannot be changed. A realistic set of parameter values (the actual values for the Intelsat IV Spacecraft) might be given as

$$\bar{I}_1 = \bar{I}_2 = 4935 \text{ lb-in.-sec}^2; \quad \bar{I}_3 = 2400 \text{ lb-in.-sec}^2$$
$$I_3' = 1634 \text{ lb-in.-sec}^2; \quad \Omega = 0; \quad \sigma = 6.28 \text{ rad/sec} \tag{29}$$

It is desired to provide nutation damping for this spacecraft by means of a small CMG semipassive damper. To keep the CMG small, let

$$J_3 = I_3'/10{,}000; \quad J_1 = J_3/1.8 \tag{30}$$

The parameters that may be varied to improve the behavior of the system are the spring constant k, the damping constant c and the CMG spinrate. The system parameters that correspond to these quantities are p^2, ζ, and η, respectively. To lend more physical significance to the results, however, the gyro angular momentum h will be used in place of η, where

$$h = (\bar{I}_1 + J_1)\eta \tag{31}$$

Two additional parameters useful in the presentation of results are $\Lambda \equiv I_3'\sigma/\bar{I}_1$ (approximately equal to the nutation or excitation frequency as seen on B) and a tuning factor $f = p^2/\Lambda^2$. As might be expected, initial calculations show that the most effective damper is obtained when $f = 1$. Thus, $p^2 = \Lambda^2$ in most of the calculations that follow. Figure 2 shows how the settling time varies when the remaining two free parameters ζ and h are varied. In view of the small additional improvement that can be achieved by going to large values of h, it was decided (arbitrarily) to use 12 in.-lb-sec as a base line value for h. (For comparison it may be noted that the system angular momentum is roughly 10,300 in.-lb-sec.) The settling time for this value of h is 4 sec. This is achieved for a ζ of 0.25.

Figure 3 shows how the settling time changes when f is varied. These results justify the selection of $f = 1$.

In Fig. 4, the gyro momentum h is held constant, but the spin axis inertia J_3 (and hence J_1 and Σ) is varied. The curves can be used to compare the effectiveness of high-speed, low-inertia gyros with low-speed, high-inertia gyros using settling time as an index. The results indicate that this is not a sensitive trade-off in the neighborhood of the baseline system. Although lifetime and reliability would also be important factors in an actual design, they are not considered here.

To evaluate the linearized analysis, the nonlinear equations of motion were integrated numerically on a digital computer. The results of one such integration is shown in Fig. 5. The nutation angle plotted on the vertical axis of Fig. 5 is the angle between X_3 and the system angular momentum. The parameter values used are those shown in Eqs. (29) and (30) plus the baseline values for p^2, ζ, and h (2.08 rad^2/sec^2, 0.25, and 12 lb-in.-sec, respectively). Although the nonlinear results are in agreement with the linear predictions for relatively small nutation angles (less than 0.5°), the gimbal angle excursions become very large for larger nutation angles, and settling times tend to increase somewhat. For example, a nutation angle of 1.0° results in gimbal excursions in excess of 70°. Although the nutation and gimbal angle still decay quite rapidly, practical considerations might require that a less highly tuned (and therefore less effective) damper be employed. Nevertheless, the platform-mounted, semipassive CMG damper appears to be an effective device.

Active Nutation Damper

Potential advantages of an active damper include increased effectiveness, freedom of location (on platform or rotor), and increased flexibility through variations of the control law. It is also possible that, because of the difficulties connected with designing, building, and testing a so-called linear dashpot, an active device would actually be easier to construct and more predictable. The sensor can be a single-degree-of-freedom translational accelerometer mounted on the body containing the damper (body B in the present development). This device is attractive because it is simple and because it is completely internal to the spacecraft. The acceleration of an arbitrary point P on B is given by

$$\begin{aligned} a^P = [&-p_1(\omega_2^2 + \omega_3^2) - p_2(\dot{\omega}_3 - \omega_1\omega_2) + \\ &p_3(\dot{\omega}_2 + \omega_1\omega_3)]\mathbf{x}_1 + [p_1(\dot{\omega}_3 + \omega_1\omega_2) - \\ &p_2(\omega_1^2 + \omega_3^2) - p_3(\dot{\omega}_1 - \omega_2\omega_3)]\mathbf{x}_2 + \\ &[-p_1(\dot{\omega}_2 - \omega_1\omega_3) + p_2(\dot{\omega}_1 + \omega_2\omega_3) - \\ &p_3(\omega_1^2 + \omega_2^2)]\mathbf{x}_3 \end{aligned} \tag{32}$$

where

$$\mathbf{p} = \sum_{i=1}^{3} p_i\mathbf{x}_i$$

is a position vector from the system mass center to P.

A single-axis translational accelerometer can measure one component of this acceleration. Suppose it is mounted parallel to X_3 to eliminate steady-state signals. Then the linear approximation of the measured acceleration a_m is

$$a_m = -p_1(\dot{\omega}_2 - \Omega\omega_1) + p_2(\dot{\omega}_1 + \Omega\omega_2) \tag{33}$$

This signal can be used to generate commands to a torque motor which in turn controls the gimbal angle γ.

The governing equation for servomotors of the type typically used in applications such as the present one may be written as[8]

$$\rho K_T e_a = J_m\rho^2\ddot{\gamma} + \beta\rho^2\dot{\gamma} + T_1 \tag{34}$$

T_1 is the X_1 component of the torque applied to the CMG by the motor [equivalent to $\mathbf{T}\cdot\mathbf{x}_1$ in Eq. (5)]. For definitions of other new symbols, please refer to the Nomenclature. In terms of T_1, the counterpart of Eq. (7) that applies for the active damper becomes

$$\begin{aligned} J_1(\dot{\omega}_1 + \ddot{\gamma}) + &(\omega_2\cos\gamma + \omega_3\sin\gamma)(-\omega_2\sin\gamma + \\ &\omega_3\cos\gamma)(J_3 - J_1) + (\omega_2\cos\gamma + \\ &\omega_3\sin\gamma)\Sigma J_3 = T_1 - c\dot{\gamma} \end{aligned} \tag{35}$$

[In Eq. (35), c represents viscous friction naturally present in the gimbal bearings and not intentionally introduced damping.] Linearizing this equation and writing it in a form similar to Eq. (8), one obtains

$$\ddot{\gamma} + (c/J_1)\dot{\gamma} + \Omega\nu\gamma = -\dot{\omega}_1 - \nu\omega_2 + T_1/J_1 \quad (36)$$

One additional relationship is required to form a complete set of equations—the relationship between the measured acceleration a_m and the armature voltage e_a. Although it may be possible to improve the performance of the system by introducing more elaborate compensation or perhaps even additional feedback loops, only amplification with a phase lag will be employed here, i.e.,

$$\tau_0\dot{e}_a + e_a = Ka_m \quad (37)$$

In this expression, K represents the gain of the accelerometer and amplifier linking the measured acceleration to the motor input voltage, and τ_0 represents the time constant of a simple lag introduced to improve performance. The value of τ_0 may also reflect the effects of inductance in the motor and other portions of the electrical circuitry. It is expected that these sources of inductance will make a very small contribution to τ_0.

Investigations to be described shortly show that the performance obtainable without additional compensation is quite satisfactory for rotor-mounted CMG dampers. Although platform mounted dampers are only considered briefly, it appears that an additional position feedback loop would be required to effectively align the rotor axis with the system angular momentum. For this reason, a passive CMG damper might be preferred if platform mounting were deemed desirable.

Reaction Torque Analysis

Small departures of the actively controlled system from the desired nominal motion are completely described by Eqs. (4a-b, 33, 34, 36, and 37). Large departures from this motion may be examined by retaining a linear model of the motor dynamics while substituting the appendix equations for Eqs. (4a-b), the X_3 component of Eq. (32) for Eq. (33), and Eq. (35) for Eq. (36). Before embarking on a direct study of these equations, a reaction torque analysis similar to that presented earlier will be discussed briefly.

Beginning as before, the right-hand sides of Eqs. (4a-b) are at first neglected. Again assuming a symmetric spacecraft, Eqs. (10) are satisfied, and ω_1 and ω_2 are given by Eq. (11). The latter equation permits calculation of a_m from Eq. (33) as

$$a_m = \omega_t(\lambda - \Omega)[-p_1 \sin\lambda t + p_2 \cos\lambda t] \quad (38)$$

By substituting this expression into Eq. (37), e_a becomes

$$e_a = \omega_t(\lambda - \Omega)K[(\lambda p_2 - p_1/\tau_0)\sin\lambda t + (\lambda p_1 + p_2/\tau_0)\cos\lambda t]/[\tau_0(\lambda^2 + \tau_0^{-2})] \quad (39)$$

The introduction of Eq. (39) into the equation obtained by eliminating T_1 from Eqs. (34) and (36) yields

$$[1 + \rho^2 J_m/J_1]\ddot{\gamma} + [(\beta\rho^2 + c)/J_1]\dot{\gamma} + \Omega\nu\gamma = A \sin\lambda t + B \cos\lambda t \quad (40)$$

where

$$A \equiv \omega_t(\lambda - \Omega)\rho K_T K(\lambda p_2 - p_1/\tau_0)/[\tau_0 J_1(\lambda^2 + \tau_0^{-2})] \quad (41a)$$

and

$$B \equiv \omega_t\left[\nu - \lambda + \frac{(\lambda - \Omega)\rho K_T K(\lambda p_1 + p_2/\tau_0)}{\tau_0 J_1(\lambda^2 + \tau_0^{-2})}\right] \quad (41b)$$

Eq. (40) is the active CMG counterpart of Eq. (12). It possesses a solution of the same form as that given in Eq. (13)

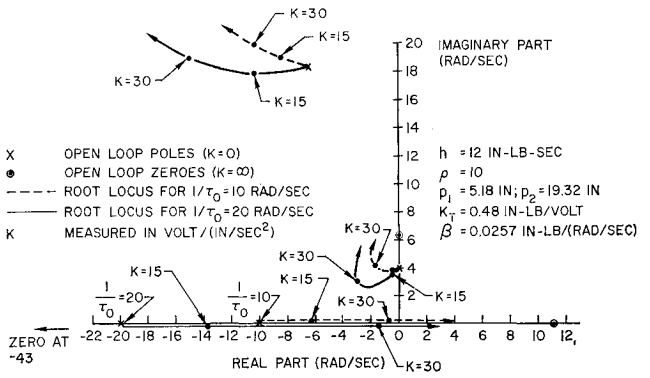

Fig. 6 Root loci for variations in K.

except now, letting $C \equiv (\beta\rho^2 + c)\lambda/J_1$, and $D \equiv \Omega\nu - (1 + J_m\rho^2/J_1)\lambda^2$,

$$\gamma_0 = [(A^2 + B^2)/(C^2 + D^2)]^{1/2} \quad (42)$$

and

$$\phi = \tan^{-1}(C/D) + \tan^{-1}(A/B) \quad (43)$$

These expressions for γ_0 and ϕ can be used to evaluate the product $(\mathbf{M}_t \cdot \boldsymbol{\omega}_t)_{\text{ave}}$ by means of Eq. (18). Because the expressions obtained for the actively controlled CMG are substantially more complicated than those obtained for the passively controlled CMG, it is not practical to develop an analytical expression for $(\mathbf{M}_t \cdot \boldsymbol{\omega})_{\text{ave}}$ similar to Eq. (19). It is, however, relatively easy to evaluate this quantity numerically when specific values are assigned to the system parameters and the nutation angle. In this way, one can obtain preliminary information regarding the stability of the system and the selection of desirable parameter values.

The reaction torque development is also useful for estimating the gimbal angle excursions, the torque supplied by the servomotor, and the rate at which electrical energy is consumed by this motor. The first of these quantities is determined by evaluating γ_0 as given in Eq. (42), and the second is determined by dividing T_1 as obtained from Eqs. (13, 34, 39, 42, and 43) by the gear ratio ρ. To find the rate of electrical energy consumption, hereafter called P (power), additional equations must be introduced.

The power P is defined as the product of e_a and the armature current i_a. Neglecting armature inductance, i_a may be shown[8] to satisfy

$$i_a = (e_a - K_e\rho\dot{\gamma})/R_a \quad (44)$$

where R_a is the armature resistance, and K_e is a constant associated with the back emf in the armature circuit. Substitution of the appropriate reaction torque solutions from Eqs. (13) and (39) into the expression for power that results when Eq. (44) is used to eliminate i_a yields, after averaging over one nutation cycle of period $2\pi/\lambda$, the following expression for the average value of P:

$$P_{\text{ave}} = E/2R_a\{(\lambda p_2 - p_1/\tau_0)[\gamma_0\rho\lambda K_e \cos\phi + E(\lambda p_2 - p_1/\tau_0)] + (\lambda p_1 + p_2/\tau_0) \times [-\gamma_0\rho\lambda K_e \sin\phi + E(\lambda p_1 + p_2/\tau_0)]\} \quad (45)$$

where $E \equiv \omega_t(\lambda - \Omega)K/\tau_0(\lambda^2 + \tau_0^{-2})$. In Eq. (45), γ_0 and ϕ are evaluated by means of Eqs. (42) and (43).

When a specific numerical example is considered later, it will be shown that these estimates of gimbal excursions, torque levels, and average power differ by only a few percent from the results of a numerical integration of the full nonlinear equations. Thus, these estimates become a valuable tool in the design of actual systems. In addition to making such estimates possible, this approximate development points out a potential shortcoming of the system as presently conceived. Namely, if the CMG is mounted on the platform (in which

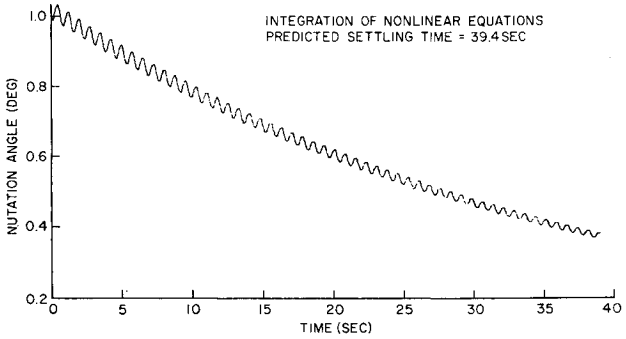

Fig. 7 Attenuation of nutation: active system.

case Ω is zero), the gimbal angle γ may not return to zero even after all coning motion of the spacecraft stops. This can be seen by examining Eq. (40) in which γ = constant becomes a possible solution when Ω and ω_t (and hence, A and B) are both zero. This behavior may be undesirable, because the presence of a small component of gyro angular momentum perpendicular to the rotor axis results in this axis being slightly displaced from the system angular momentum vector even though the platform is motionless.

This deficiency could be corrected by introducing either an additional position feedback loop or a mechanical spring to drive the gimbal angle to zero at the same time as the rotor axis converges on the angular momentum vector. The development that follows, however, is concerned primarily with rotor-mounted CMG's, and since no such modification is required for a rotor-mounted CMG, this question will not be pursued further at this time. As will be shown, the substitution of specific parameter values into the expressions generated in this section indicates that an actively controlled, rotor-mounted CMG is an effective device for attenuating nutation.

Linearized Analysis

Equations (4a-b, 33, 34, 36, and 37) form a complete set of linear, constant coefficient differential equations governing small motions of the system. The characteristic equation for this set is

$$s^5 + a_4 s^4 + a_3 s^3 + a_2 s^2 + a_1 s + a_0 = 0 \tag{46}$$

where if δ_1 thru δ_8 are defined as

$$\begin{gathered}\delta_1 \equiv Kp_1; \quad \delta_2 \equiv Kp_2; \quad \delta_3 \equiv \Omega(\eta - \Delta\Omega) \\ \delta_4 \equiv r(\eta - 2\Delta\Omega); \quad \delta_5 \equiv \nu\Omega; \quad \delta_6 \equiv \rho K_T/J_1 \\ \delta_7 \equiv J_m\rho^2/J_1; \quad \delta_8 \equiv (\beta\rho^2 + c)/J_1\end{gathered} \tag{47}$$

then

$$a_0 = \lambda_2[\delta_3(\Omega\delta_2\delta_6 - \nu) + \delta_5\lambda_1]/[\tau_0(1 + \delta_7 - \Delta)] \tag{48a}$$

$$a_1 = [-\lambda_2\delta_3(\delta_1\delta_6 + \tau_0\nu) + \delta_1\delta_6\Omega(\delta_3 + \lambda_1\delta_4) + \lambda_1\lambda_2(\tau_0\delta_5 + \delta_8)]/[\tau_0(1 + \delta_7 - \Delta)] \tag{48b}$$

$$a_2 = [(-\delta_2\delta_6\Omega + \nu)(-\Delta\lambda_2 + \delta_4) - \delta_3(1 - \delta_2\delta_6) - \lambda_1\delta_4(1 - \delta_2\delta_6) + \lambda_1\lambda_2(1 + \delta_7 + \tau_0\delta_8) + \delta_5]/[\tau_0(1 + \delta_7 + \Delta)] \tag{48c}$$

$$a_3 = \{(\delta_1\delta_6 + \tau_0\nu)(\delta_4 - \Delta\lambda_2) + \Delta\Omega\delta_1\delta_6 - \tau_0(\delta_3 - \delta_5) + \tau_0\lambda_1[\lambda_2(1 + \delta_7) - \delta_4] + \delta_8\}/[\tau(1 + \delta_7 - \Delta)] \tag{48d}$$

$$a_4 = [\Delta(-1 + \delta_2\delta_6) + 1 + \tau_0\delta_8 + \delta_7]/[\tau(1 + \delta_7 - \Delta)] \tag{48e}$$

The relatively high order of this equation and the complexity of its coefficients make it impractical to generate a set of analytical stability criteria for this system. Its behavior, therefore, will be studied numerically by means of root locus techniques. Before embarking on this investigation, it is worth noting that when $\Omega = 0$ (i.e., the CMG is mounted on the despun platform), $a_0 = 0$ also, making $s = 0$ a root of the characteristic equation. A zero root means the nominal motion is not asymptotically stable and reflects the behavior discussed earlier where it was observed on the basis of reaction torque arguments that an actively controlled CMG will not function effectively on the despun platform without some modification. Although this observation has little impact on the remaining development, a development which deals exclusively with rotor-mounted CMG's, it does demonstrate a general agreement between reaction torque analysis and more rigorous analyses.

For numerical investigations of the actively controlled CMG system, we use the same $\bar{I}_1 = \bar{I}_2$ and $\bar{I}_3$ as before [Eqs. (29)], but

$$I_3' = 766 \text{ lb-in.-sec}^2, \ \Omega = -\sigma = 6.28 \text{ rad/sec} \tag{49}$$

because of the placement of the CMG on the rotor instead of the platform. As regards the gyro parameters, it is assumed following the previous work that

$$J_3 = (\bar{I}_3 - I_3')/10{,}000; \quad J_1 = J_3/1.8 \tag{50}$$

$$h = (\bar{I}_1 + J_1)\eta = 12 \text{ lb-in.-sec} \tag{51}$$

The damping constant c representing gimbal friction is assumed negligibly small, and the gear ratio ρ is taken as 10. The relevant motor constants, chosen to represent a commercially available servomotor weighing approximately 6 lb, are given by

$$\begin{gathered}K_T = 0.48 \text{ in.-lb/v}; \quad \beta = 0.0257 \text{ in.-lb/(rad/sec)} \\ R_a = 0.97 \text{ ohm}; \quad J_m = 0.0011 \text{ lb-in.-sec}^2\end{gathered} \tag{52}$$

The parameters that remain unspecified are p_1 and p_2, which depend on the location of the accelerometer, the gain K of the accelerometer-amplifier, and the compensation time constant τ_0. Normally, the designer would be free to select values for these parameters (subject to certain physical limitations) that optimize the performance of the system. To investigate the relationship between these parameters and performance, an algorithm for computing the roots of the characteristic equation was programed on a digital computer. Initial explorations revealed (as expected on the basis of reaction torque arguments) that the location of the accelerometer was an important consideration, values of p_1/p_2 near cot75° being found desirable for attenuating nutation rapidly. With p_1/p_2 fixed at this value, K and τ_0 were varied systematically. The results of these investigations are summarized in Fig. 6, where p_1 and p_2 are taken as

$$p_1 = 20(\cos 75°) = 5.18 \text{ in.}; \quad p_2 = 20(\sin 75°) = 19.32 \text{ in.} \tag{53}$$

and K is varied between 0 and 30 v/(in./sec^2) for $\tau_0 = 1/10$ sec and $\tau_0 = 1/20$ sec. The figure shows that for a given value of K, the roots nearest the imaginary axis are more highly damped when τ_0 is 1/20 sec than when τ_0 is 1/10 sec.

Additional factors such as gimbal angle excursions, torque levels, and power consumption must be considered in selecting a final design. When these quantities are estimated using reaction torque analyses, it may be found that the more highly damped roots represent larger gimbal angles and greater power consumption, so that difficult trade-offs have to be weighed in a realistic case. Since the purpose of this investigation is primarily to demonstrate the efficacy of the proposed control scheme and not to provide a detailed design, further studies to choose appropriate values for K and τ_0 were carried out only until reasonably acceptable perform-

ance was obtained. Recognizing that further improvements could undoubtedly be made for specific designs, we assigned the values

$$K = 1.25 \text{ v/(in./sec}^2\text{)}; \quad \tau_0 = \tfrac{1}{20} \text{ sec} \tag{54}$$

With the remaining system parameters satisfying Eqs. (49–53), the predicted settling time obtained by examining the roots of the characteristic equation is 39.4 sec, and the estimated gimbal angle excursion, torque amplitude, and average power consumption for 1° of nutation are 33°, 4.6 in.-lb, and 45.8 w, respectively (estimates based on reaction torque analyses). These values strongly reflect the magnitude of the nutation angle, and will decrease as that angle decreases.

Nonlinear Verification

To evaluate the accuracy and utility of the predictions and procedures just described, the full nonlinear equations (with linear motor dynamics) were again integrated on a digital computer. The results for parameter values satisfying Eqs. (49–54) and an initial nutation angle of 1° are shown in Fig. 7. The actual settling time as determined from Fig. 7 is virtually identical to its predicted value. The gimbal angle excursions, torque amplitude, and average power determined from the nonlinear integration were found to agree with their corresponding estimated values to within 6% at 1° of nutation. Better agreement was found for smaller nutation angles.

Summary

It has been demonstrated that well-designed semipassive and active mechanisms employing CMG's can very effectively attenuate the coning of a dual-spin spacecraft. For a semipassive device, platform mounting is required, but for an active device rotor mounting is also possible. In providing analytical support for these statements, ways have been shown in which heuristic reaction torque arguments, linear analysis, and numerical integration can be effectively combined to obtain increased understanding of the important features of the behavior of these systems.

Appendix: Nonlinear Equations of Motions—System Equations

$$(\bar{I}_1 + J_1)\dot{\omega}_1 + J_1\ddot{\gamma} + (J_1 - J_3)c\gamma s\gamma(\omega_2^2 - \omega_3^2) + [\bar{I}_3 - \bar{I}_2 + (J_3 - J_1)(c^2\gamma - s^2\gamma)]\omega_2\omega_3 + (I_3'\sigma + J_3\Sigma c\gamma)\omega_2 + J_3\Sigma s\gamma\omega_3 = 0$$

$$(\bar{I}_2 + J_1c^2\gamma + J_3s^2\gamma)\dot{\omega}_2 + (J_1 - J_3)c\gamma s\gamma(\dot{\omega}_3 - \omega_1\omega_2) + [\bar{I}_1 - \bar{I}_3 + (J_1 - J_3)c^2\gamma]\omega_1\omega_3 + 2(J_3 - J_1)c\gamma s\gamma\omega_2\dot{\gamma} + [2J_1c^2\gamma + J_3(s^2\gamma - c^2\gamma)]\omega_3\dot{\gamma} - (I_3'\sigma + J_3\Sigma c\gamma)\omega_1 - J_3\Sigma c\gamma\dot{\gamma} = 0$$

$$(\bar{I}_3 + J_1s^2\gamma + J_3c^2\gamma)\dot{\omega}_3 + (J_1 - J_3)c\gamma s\gamma(\dot{\omega}_2 + \omega_1\omega_3) + [\bar{I}_2 - \bar{I}_1 + (J_3 - J_1)s^2\gamma]\omega_1\omega_2 + [J_3(s^2\gamma - c^2\gamma) - 2J_1s^2\gamma]\omega_2\dot{\gamma} + 2(J_1 - J_3)c\gamma s\gamma\omega_3\dot{\gamma} - J_3\Sigma s\gamma(\omega_1 + \dot{\gamma}) = 0$$

where $s\gamma \equiv \sin\gamma$ and $c\gamma \equiv \cos\gamma$.

References

[1] Landon, V. D. and Stewart, B., "Nutational Stability of an Axisymmetric Body Containing a Rotor," *Journal of Spacecraft and Rockets*, Vol. 1, No. 6, Nov.-Dec. 1964, pp. 682–684.

[2] Iorillo, A. J., "Nutation Damping Dynamics of Axisymmetric Rotor Stabilized Satellites," presented at the American Society of Mechanical Engineers, Winter Meeting, Nov. 1965.

[3] Likins, P. W., "Attitude Stability Criteria for Dual Spin Spacecraft," *Journal of Spacecraft and Rockets*, Vol. 4, No. 12, Dec. 1967, pp. 1638–1643.

[4] Mingori, D. L., "Effects of Energy Dissipation on the Attitude Stability of Dual-Spin Satellites," *AIAA Journal*, Vol. 7, No. 1, Jan. 1969, pp. 20–27.

[5] *Proceedings of the Symposium on Attitude Stabilization and Control of Dual-Spin Spacecraft*, TR 0158(3307-01)-16, Nov. 1967, Aerospace Corp., El Segundo, Calif., pp. 73–109; also Rept. SAMSO-TR-68-191, U.S. Air Force.

[6] Cloutier, G. J., "Nutation Damper Design Principles for Dual-Spin Spacecraft," *Journal of the Astronautical Sciences*, Vol. XVI, No. 2, March-April 1969, pp. 79–87.

[7] Kane, T. R. and Scher, M. P., "A Method of Active Attitude Control Based on Energy Considerations," *Journal of Spacecraft and Rockets*, Vol. 6, No. 5, May 1969, pp. 633–636.

[8] Clark, R. N., *Introduction to Automatic Control Systems*, Wiley, New York, 1962, pp. 44–59.